Noncollinear Optical Frequency Doubling in Strontium Barium Niobate

Arthur R. Tunyagi, Michael Ulex, and Klaus Betzler*
Fachbereich Physik, Universität Osnabrück, D-49069 Osnabrück, Germany

(Received 18 February 2003; revised manuscript received 21 April 2003; published 20 June 2003)

The observation of a novel noncollinear optical second-harmonic generation mechanism is reported. In strontium barium niobate crystals, a circular cone of second-harmonic light is generated when a fundamental beam of intensive laser light is directed along the crystallographic *c* axis. It can be shown that the effect is caused by the nonlinear polarization of antiparallel ordered ferroelectric microdomains.

DOI: 10.1103/PhysRevLett.90.243901 PACS numbers: 42.65.Ky, 42.70.Mp, 77.84.Dy

Optical frequency doubling—second-harmonic generation (SHG)—is widely used to generate intense coherent light in wavelength regions not accessible by conventional lasers (far ultraviolet) or in regions where it has an efficiency advantage (frequency doubling of diode pumped solid state lasers). To achieve a large interaction length between exciting fundamental waves and generated harmonic waves, in general *collinear* arrangements are used, i.e., the wave vectors of fundamental and harmonic waves are parallel to each other. Furthermore, so-called phase matching between fundamental and harmonic wave is adjusted in order to maximize the second-harmonic intensity—the momentum conservation law is fulfilled:

$$k_2 = k_1 + k_1'. \tag{1}$$

In Eq. (1), k_1 and k_1' are the wave vectors of the fundamental waves, k_2 of the harmonic one, respectively, inside the nonlinear medium used for SHG. This strong momentum conservation rule may be relaxed using so-called quasiphase matching, a technique originally proposed by Bloembergen and now applied in various practical nonlinear optical crystals.

On the other hand, many scenarios for *noncollinear* interactions are known in connection with SHG. These include several scattering mechanisms such as hyper-Raman and hyper-Rayleigh or scattering of the second harmonic at inhomogeneities of the refractive index [1]. Phononless, direct noncollinear frequency doubling—induced [2] or spontaneous [3]—can be used for the spatially resolved characterization of electro-optic and nonlinear optical materials [4]. Furthermore, noncollinear effects may enter by wave mixing, as e.g., four-wave mixing [5,6]. Recently, a novel class of noncollinear processes was described by Moll *et al.* [7] which utilizes higher order nonlinearities to generate cones of lower order harmonics. In all these interactions, momentum conservation is fulfilled in a *noncollinear* way, Eq. (1) or its appropriate extension in the case of more waves involved has to be interpreted then in a vectorial sense. Moreover, often an additional momentum k_q of the additional participating quasiparticles (e.g., phonons) has to be included. Because of the lack of coherence or due to the limited interaction volume, in all noncollinear schemes the second-harmonic intensities are low compared to the collinear ones.

In this Letter, we report on a novel noncollinear mechanism which we detected in crystals of strontium barium niobate (SBN)—cone-shaped second-harmonic generation when illuminating the crystals parallel to their polar *c* axis.

Using the Czochralski method, SBN crystals (the chemical formula is $Sr_xBa_{1-x}Nb_2O_6$) can be grown in a wide composition range spanning approximately $x = 0.3, \ldots, 0.8$ [8,9]. A congruently melting composition, yielding crystals of high homogeneity, has been determined to be at $x \approx 0.61$ [10]. At room temperature, undoped crystals of all compositions are ferroelectric with the tetragonal space group *P4bm* [11]. Because of this symmetry, two directions of the ferroelectric polarization are allowed, parallel and antiparallel to the crystallographic *c* axis. At higher temperatures the crystals undergo a phase transition into a tetragonal paraelectric phase which is centrosymmetric. The symmetry of the noncentrosymmetric ferroelectric phase of SBN forces the nonlinear susceptibility tensor for SHG to be of the form

$$d_{ij} = \begin{pmatrix} 0 & 0 & 0 & 0 & d_{15} & 0 \\ 0 & 0 & 0 & d_{24} & 0 & 0 \\ d_{31} & d_{32} & d_{33} & 0 & 0 & 0 \end{pmatrix} \tag{2}$$

with $d_{31} = d_{32}$ and $d_{15} = d_{24}$. From the nonzero elements in the tensor it can be deduced that the generation of second-harmonic light is possible only in a geometry where at least one of the three participating light waves has a polarization component parallel to the crystallographic *c* axis.

In our experiments we directed an unexpanded laser beam with low divergence (pulsed Nd:YAG at a wavelength of 1064 nm, 5 ns pulse length, 10 kW peak power, 1 kHz repetition rate) onto a thin sample (≈0.8 mm) of SBN. As a sample an optically homogeneous piece of a crystal grown from the congruently melting composition (strontium content $x = 0.61$) was selected. The direction

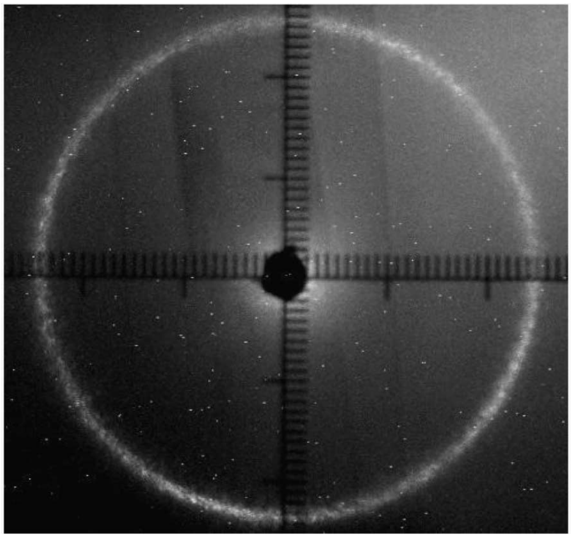

FIG. 1. Circular ring of second-harmonic light generated by a fundamental beam directed along the crystallographic c axes in SBN. The distance between the crystal and the projection screen is 25 mm, the ring diameter at the screen approximately 50 mm. The near-infrared fundamental beam is visible as a bright central spot due to the sensitivity of the camera in this spectral region.

of the fundamental beam (k_1, k_1') was chosen parallel to the crystallographic c axis. As expected from the tensor components, no second-harmonic light in the direct beam direction was generated. Yet, instead, a cone of green SHG light (532 nm) was produced, showing up as a circular ring on the projection screen (Fig. 1).

The polarization of the second-harmonic light in this cone is radial; Fig. 2 shows the principle. This radial polarization behavior is completely unaffected by the polarization of the fundamental beam. Both, the radial second-harmonic polarization and its independence from the fundamental beam, conform with the symmetry of the SHG tensor [Eq. (2)].

Similar ring-shaped patterns are found in a vast variety of so-called parametric scattering processes in photorefractive crystals [12–14]. Although SBN is one of the most interesting photorefractive materials, parametric scattering in combination with harmonic generation can be excluded as an explanation due to two main reasons. First, the photorefractive response of a material arises from suitable impurities; we used undoped crystals. Second, the onset of parametric scattering processes always shows a temporal evolution. To check this point, we measured the time shape of the ring signal at the very first laser pulse and at the 5000th, i.e., after 5 s, using a photomultiplier. The oscilloscope traces of these two signals are depicted in Fig. 3. They are nearly identical, thus parametric scattering processes can be clearly excluded.

In a spectral analysis of the second-harmonic light we found no wavelength shift which would indicate a phonon participation in the process. Because of the limited spectral resolution, yet, low energetic (acoustic) phonons cannot be excluded thereby. Any phonon participation, however, would relax the momentum condition considerably, thus preventing an expressed pattern.

Several authors have demonstrated that micrometer-sized needlelike domains play an important role for light scattering and for the type of the phase transition in SBN [1,15–17]. These domains are in antiparallel order; the ferroelectric polarization is parallel or antiparallel to the crystallographic c direction. To prove whether these domains also are responsible for the noncollinear second-harmonic process, we poled a sample by cooling it down from the high-temperature paraelectric phase with an electric field applied in the c direction. After that the ring structure had vanished. This is also a strong indication that higher nonlinearities of odd order [7] which are insensitive to poling and the corresponding symmetry aspects do not contribute to the effect. Having thus proven that antiparallel ferroelectric domains are the basic cause for the noncollinear SHG effect, we carried out model calculations based on antiparallel domains to explain the ring structure.

Plane light waves propagating along the c direction of SBN contain only electric field components perpendicular to this direction, E_1 and E_2. According to the shape of the SHG tensor for SBN, these field components produce a second order nonlinear polarization P_3. The sign of P_3 depends on the domain orientation, here indicated by arrows:

$$P_3(\Uparrow) = d_{31}E_1E_1 + d_{32}E_2E_2, \tag{3}$$

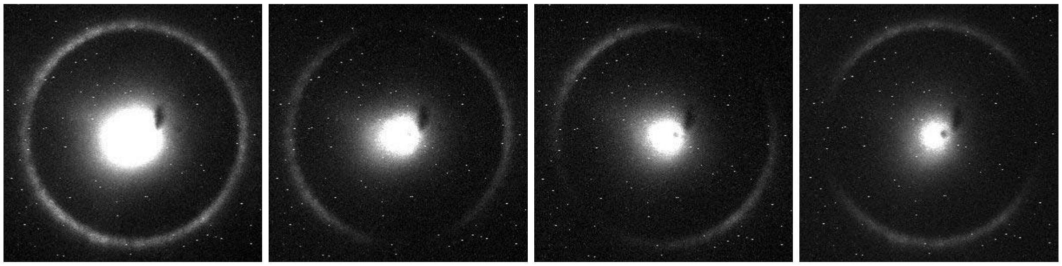

FIG. 2. Polarization properties of the SHG ring. From left to right: without analyzer, analyzer oriented horizontal, analyzer at 45°, analyzer oriented vertical. The bright central spot is due to the infrared fundamental beam.

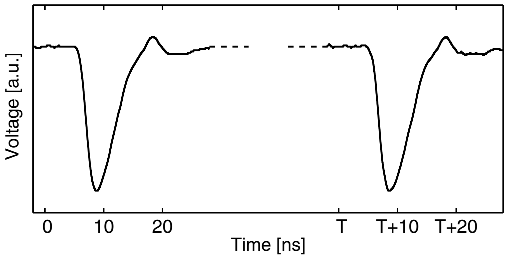

FIG. 3. Oscilloscope traces of the ring intensity (photomultiplier signal) at the first and at the 5000th pulse of the exciting laser. The pulse width is approximately 5 ns, the time T between the two pulses shown here is 5 s.

$$P_3(\Downarrow) = -d_{31}E_1E_1 - d_{32}E_2E_2. \tag{4}$$

For simplicity, all oscillatory factors have been omitted from E and P. E may be assumed to be monochromatic at frequency ω, P accordingly at 2ω. The induced second-harmonic polarization P_3 acts as a source for dipolar radiation at this frequency 2ω.

The simplest nontrivial arrangement of domains contains just two antiparallel ordered ones. For the calculation, the domain sizes were assumed to be on the order of the second-harmonic wavelength. To compute the far-field behavior, the domains were replaced by suitable dipolar point sources. The angular intensity distribution due to the interference of the respective dipolar radiation fields is schematically sketched in Fig. 4 for the plane defined by the two dipole vectors.

No intensity in the forward direction, instead a broad angular intensity distribution around two distinct angles symmetric to the c direction is found. The dominant angles are determined by the domain sizes. Because of the oscillation direction of the dipoles, the polarization of the second-harmonic light is in the plane shown.

Increasing the number of equally sized domains leads to a narrowing of this angular distribution. Yet in real crystals it cannot be expected that one deals with ideal equally sized domains. We therefore generalized the calculational scheme and calculated the angular intensity distribution for a planar arrangement of short domains with a random distribution of the widths. For the calculations, the domains were replaced by appropriate dipolar point sources. A typical result is shown in Fig. 5.

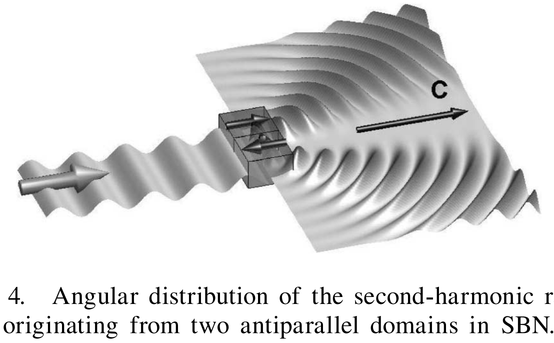

FIG. 4. Angular distribution of the second-harmonic radiation originating from two antiparallel domains in SBN. The exciting wave propagates in the c direction from the left side.

Again, the polarization of the second-harmonic light is *in plane*. Varying the random distribution of the domain widths varies the random fine structure of the intensity distribution; the common features, however—no intensity in the forward direction and a broad angular distribution starting at approximately 10°—are maintained. Extending the model to an arrangement of needlelike long domains, means, as pointed out earlier, that, in addition to the calculated angular distribution of Fig. 5, strong momentum conservation has to be obeyed, yielding

$$k_2 = k_1 + k_1' + k_g. \tag{5}$$

Here, k_g represents any spatial periodicity present in the domain arrangement, $k_1 = k_1'$ characterizes the fundamental beam in the c direction, and k_2 one of the harmonic waves. Because of the random distribution of domain widths, k_g shows up a corresponding reciprocal distribution. The direction of k_g, however, is strictly perpendicular to the c axis according to the extent of the domains in the c direction. The momentum geometry for the phase-matching condition of Eq. (5) is sketched in Fig. 6.

The angle Θ between fundamental and harmonic wave vectors inside the crystal is defined by

$$\cos\Theta = \frac{k_1 + k_1'}{k_2} = \frac{n^o(\omega)}{n^e(\Theta, 2\omega)}. \tag{6}$$

Using the refractive index data published for SBN [18], Eq. (6) yields an internal angle Θ of 17.1°, corresponding to an external angle of 44.8°. This is in excellent agreement with the measured angle, 45 ± 1°, derived from Fig. 1.

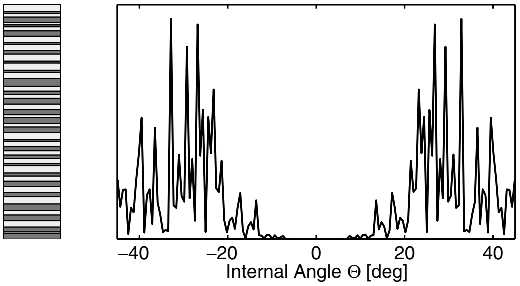

FIG. 5. Angular distribution of the second-harmonic light intensity arising from a planar array of 200 *randomly sized* antiparallel ordered domains in SBN. A part of the domain arrangement is sketched on the left side: the c direction is horizontal, the dark domains are polarized parallel, the light ones antiparallel to this direction, and the exciting wave propagates in the c direction.

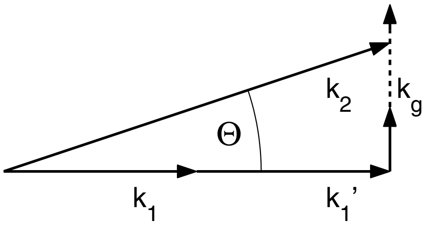

FIG. 6. Momentum diagram for Eq. (5). k_1 and k_1' are in the c direction, k_g is perpendicular to it with a distribution as indicated by the dashed line.

The extension of the model to a three-dimensional arrangement of needlelike long domains with randomly distributed widths is straightforward. Angular intensity distribution and the phase-matching condition of Eq. (5) lead to a cone of second-harmonic light with an internal cone angle Θ. *In-plane* polarization for all radial directions then accounts for the *radial* polarization experimentally found in the ring. Spatial intensity fluctuations in the ring pattern may be referred to the spatially varying random fine structure in the angular distribution.

In conclusion, we have reported on a novel mechanism for noncollinear generation of second-harmonic light in ferroelectric crystals. Antiparallel polarized long domains of random width lead to a cone-shaped SHG light emission when an intense laser beam is directed parallel to the polar axis of the crystal. The cone angle is defined by the refractive indices for fundamental and harmonic wavelengths. The light polarization in the cone is radial and is not affected by the polarization of the incident laser beam.

The authors thank T. Volk for useful advice and fruitful discussions. Support from the Graduate College *Nonlinearities of Optical Materials*, financed by the Deutsche Forschungsgemeinschaft and the Federal State of Niedersachsen, is gratefully acknowledged.

*Electronic address: Klaus.Betzler@uos.de

[1] S. Kawai, T. Ogawa, H. S. Lee, R. C. DeMattei, and R. S. Feigelson, Appl. Phys. Lett. **73**, 768 (1998).
[2] A. Reichert and K. Betzler, J. Appl. Phys. **79**, 2209 (1996).
[3] K.-U. Kasemir and K. Betzler, Appl. Phys. B **68**, 763 (1999).
[4] A. Reichert, K. U. Kasemir, and K. Betzler, Ferroelectrics **184**, 21 (1996).
[5] R. Magnusson and T. K. Gaylord, Appl. Opt. **13**, 1545 (1974).
[6] B. Sturman, M. Y. Goulkov, and S. G. Odoulov, J. Opt. Soc. Am. B **13**, 577 (1996).
[7] K. D. Moll, D. Homoelle, A. L. Gaeta, and R.W. Boyd, Phys. Rev. Lett. **88**, 153901 (2002).
[8] A. A. Ballman and H. Brown, J. Cryst. Growth **1**, 311 (1967).
[9] J. C. Brice, O. F. Hill, P. A. C. Whiffin, and J. A. Wilkinson, J. Cryst. Growth **10**, 133 (1971).
[10] K. Megumi, N. Nagatsuma, Y. Kashiwada, and Y. Furuhata, J. Mater. Sci. **11**, 1583 (1976).
[11] P. B. Jameson, S. C. Abrahams, and J. L. Bernshtein, J. Chem. Phys. **42**, 5048 (1968).
[12] B. Sturman, S. G. Odoulov, and M. Y. Goulkov, Phys. Rep. **275**, 199 (1996).
[13] L. Solymar, D. J. Webb, and A. Grunnet-Jepsen, *The Physics and Applications of Photorefractive Materials* (Clarendon Press, Oxford, 1996).
[14] M. Goulkov, S. Odoulov, I. Naumova, F. Agulló-Lopez, G. Calvo, E. Podivilov, B. Sturman, and V. Pruneri, Phys. Rev. Lett. **86**, 4021 (2001).
[15] Y. G. Wang, W. Kleemann, T. Woike, and R. Pankrath, Phys. Rev. B **61**, 3333 (2000).
[16] W. Kleemann, P. Licinio, T. Woike, and R. Pankrath, Phys. Rev. Lett. **86**, 6014 (2001).
[17] P. Lehnen, W. Kleemann, T. Woike, and R. Pankrath, Phys. Rev. B **64**, 224109 (2001).
[18] T. Woike, T. Granzow, U. Dörfler, C. Poetsch, M. Wöhlecke, and R. Pankrath, Phys. Status Solidi (a) **186**, R13 (2001).